The design and imaging characteristics of dynamic, solid-state, flat-panel x-ray image detectors for digital fluoroscopy and fluorography

A.R. Cowen[a,*], A.G. Davies[a], M.U. Sivananthan[b]

[a]LXi_Research, The University of Leeds, Division of Medical Physics, and [b]Department of Cardiology, Yorkshire Heart Centre, The General Infirmary, Leeds, West Yorkshire, UK

Dynamic, flat-panel, solid-state, x-ray image detectors for use in digital fluoroscopy and fluorography emerged at the turn of the millennium. This new generation of dynamic detectors utilize a thin layer of x-ray absorptive material superimposed upon an electronic active matrix array fabricated in a film of hydrogenated amorphous silicon (a-Si:H). Dynamic solid-state detectors come in two basic designs, the indirect-conversion (x-ray scintillator based) and the direct-conversion (x-ray photoconductor based). This review explains the underlying principles and enabling technologies associated with these detector designs, and evaluates their physical imaging characteristics, comparing their performance against the long established x-ray image intensifier television (TV) system. Solid-state detectors afford a number of physical imaging benefits compared with the latter. These include zero geometrical distortion and vignetting, immunity from blooming at exposure highlights and negligible contrast loss (due to internal scatter). They also exhibit a wider dynamic range and maintain higher spatial resolution when imaging over larger fields of view. The detective quantum efficiency of indirect-conversion, dynamic, solid-state detectors is superior to that of both x-ray image intensifier TV systems and direct-conversion detectors. Dynamic solid-state detectors are playing a burgeoning role in fluoroscopy-guided diagnosis and intervention, leading to the displacement of x-ray image intensifier TV-based systems. Future trends in dynamic, solid-state, digital fluoroscopy detectors are also briefly considered. These include the growth in associated three-dimensional (3D) visualization techniques and potential improvements in dynamic detector design.
© 2008 The Royal College of Radiologists. Published by Elsevier Ltd. All rights reserved.

Introduction

Diagnostic and interventional radiology have a continuing requirement for dose-efficient x-ray-based modes of imaging to visualize moving anatomical structures, organs and/or clinical devices (e.g., guide-wires, catheters, stents, pacemakers, etc).[1] Historically, real-time dynamic imaging using x-rays (for the purpose of procedural guidance) has been referred to as "fluoroscopy". The serial acquisition of x-ray images of higher quality for use in diagnosis and documentation is known as "fluorography". Such imaging techniques are commonly associated with contrast medium aided examinations of the gastrointestinal (GI) tract, the cardiovascular system, and various other soft-tissue organs and structures. During the second half of the 20th century fluoroscopy has been supported by the electronic imaging device known as the x-ray image intensifier television (IITV) system. Such a system comprises a chain of electron-optical imaging components including an x-ray image intensifier tube, suitable coupling lenses plus a high specification closed-circuit television

* Guarantor and correspondent: A.R. Cowen, LXi_Research, The University of Leeds, Division of Medical Physics, Worsley Building, Clarendon Way, Leeds LS2 9JT, West Yorkshire, UK. Tel.: +44 0113 3438312.
E-mail address: a.r.cowen@leeds.ac.uk (A.R. Cowen).

channel combined with a suitable electronic display.[2] The TV image is either recorded by an electronic camera tube (e.g., a Plumbicon, Saticon, Chalnicon, etc) or a semiconductor charge-coupled device (CCD) sensor.[3] Modern IITV fluoroscopy systems are capable of producing good-quality, dynamic x-ray images with economical use of radiation dose.

The emergence of digital subtraction angiography (DSA) imaging equipment circa 1980 pioneered the integration of computerized video processors and magnetic storage discs with x-ray IITV systems.[4] The success of DSA fuelled a seminal era in the development of digital fluoroscopy/fluorography equipment, which continued through the 1990s. The availability of user-friendly, high-performance, digital x-ray IITV systems led to a radical shift in clinical imaging practice. This included the replacement of spot-film-based recording of clinical results by digital (computerized) fluorography in the screening room. This made it possible to access and replay sequences of fluorographic images on-line, and to view them in a digitally enhanced form. At the same time there was an enthusiastic adoption of radiation dose-saving measures, such as digital recursive filtering (to ameliorate noise), last image hold and two-dimensional (2D) road-mapping, further increasing the clinical usefulness of digital fluoroscopy.[5] Digital x-ray IITV systems proved flexible and effective platforms for expanding the range of dynamic image acquisition protocols. Digital x-ray IITV systems have been a crucial (albeit largely unsung) enabling technology in modern radiology. Notably they have underpinned the growth in x-ray image-guided interventional radiology. At the turn of the new millennium, the digital x-ray IITV system was the dominant image receptor not only for routine fluoroscopy, but also dynamic x-ray image acquisition in general. Around this time, however, a new generation of dynamic image detectors first appeared, which has subsequently gone on to threaten the established role of digital x-ray IITV systems.

Solid-state, flat-panel detectors were originally designed for use in standard projection radiography; the basic physical and technical characteristics of these devices were described in the preceding review.[6] Solid-state digital radiography (DR) detectors provide on-line access to the electronic signal data, so the radiographic images are available to view in a matter of seconds after the exposure, (rather than after delays of several minutes more typical of conventional and computed radiography). Significantly, researchers found that with suitable technical optimization these solid-state detectors can be used equally well to record and read-out images at rates high enough to support fluoroscopy.[7,8] Prototype clinical dynamic solid-state detector systems started to appear toward the end of the 1990s.[9—15] The first commercial solid-state detector-based digital fluoroscopy products became available in 2001; these detectors were designed specifically for cardiac imaging.[16—18] In recent years most new cardiac catheterization laboratories have utilized solid-state detectors, ousting digital x-ray IITV from one of its most celebrated clinical roles. With the recent introduction of dynamic, solid-state detectors of larger area, a similar shift away from digital x-ray IITV systems is now occurring in radiography and fluoroscopy and vascular imaging.[19—25] The aim of this review is to describe the physical design and imaging characteristics of the dynamic, solid-state, flat-panel x-ray image detectors that are driving this trend.

Dynamic x-ray detector design

Currently, the majority of dynamic solid-state detectors in clinical use are based upon the so-called "indirect conversion principle".[6] These detectors exploit the conversion of x-ray energy to light photons in a layer of thallium-activated caesium iodide (CsI:Tl). The emitted light is then converted to an electronic signal in a 2D array of light-sensitive elements (i.e., photodiodes), fabricated in a thin layer of hydrogenated amorphous silicon (a-Si:H). CsI:Tl is a very similar scintillator to the CsI:Na used in x-ray image intensifier tubes. Caesium and iodine have comparatively high atomic numbers [$Z = 55$ and 53, respectively], and as such have good x-ray absorption properties. Additionally they exhibit a boost in x-ray absorption at photon energies exceeding their k-edges, at 36 and 33 keV for caesium and iodine, respectively. This ensures efficient absorption of x-ray photons over the energy range that is most relevant to fluoroscopy and fluorography. The CsI:Tl layer has a columnar (pillar-like) crystal microstructure. Consequently, this phosphor has a high packing density ($\sim$90%), again helping to maximize x-ray absorption. The channelled (fibre-optic like) micro-structure of CsI:Tl helps minimize scatter of the fluorescent light emission. As a result, comparatively thick layers of scintillator can be employed before spatial resolution is degraded significantly. For dynamic x-ray imaging applications a relatively thick CsI:Tl layer (typically 550—650 μm) is used to maximize detector sensitivity (and, therefore, minimize patient dose). The CsI:Tl layer absorbs

80−90% of the incident x-ray photons. Each x-ray photon absorbed in CsI:Tl yields ∼3×10^3 light photons, predominantly in the green portion of the optical spectrum. Of these light photons, approximately half are recorded by the 2D array of photodiodes and contribute to the electronic signal. The scintillator is grown or mounted (depending on the detector design) on top of the a-Si:H active matrix array. A light reflector may be coated on the top surface of the CsI:Tl to minimize the loss of fluorescent light and to maximize signal gain (albeit at the cost of reduced spatial resolution).

Solid-state, digital fluoroscopy systems utilize pulsed-mode x-ray exposure. In this mode the detector is exposed to a sequence of moderate to high intensity x-ray pulses of short duration (∼5−20 ms depending upon the type of examination and patient size). Pulsed-mode fluoroscopy requires a powerful grid-controlled x-ray source. This enables the pulses of radiation to be delivered rapidly and precisely, and as a result, motion-linked artefacts and unsharpness (blur) are kept to a minimum.[26] Each succeeding x-ray pulse produces fluorescent light that illuminates the photodiode array releasing electrical charge carriers that are (temporarily) stored in the matrix array. The magnitude of the charge packet stored at a particular pixel is proportional to the dose absorbed at that location. Each pixel in the active matrix array comprises a photodiode plus an associated thin film transistor (TFT) switch. The 2D array of TFT switches are addressed sequentially via a set of (horizontal) gate control lines. The signal information is, therefore, read out line-by-line to the external circuitry via a set of (vertical) data transfer lines. Fluoroscopic image frames are typically acquired at rates of up to 30 frames s^{-1}. Where clinical circumstances permit the frame rate can be reduced to 15 or 7.5 frames s^{-1} (or even lower) to moderate patient dose. The output signal is then amplified prior to digitization and transfer to the system computer. Dynamic sequences of images are finally viewed on a suitable display device in the procedure room, or at a separate viewing station.

Alternatively, dynamic, solid-state detectors can be designed to directly convert x-ray energy to electronic charge. This detector utilizes a layer of a-Se x-ray photo-conductor superimposed upon the a-Si:H active matrix.[6] The latter comprises a 2D array of charge-sensing electrodes, storage capacitors, and TFT switches. Although the density of a-Se is similar to that of CsI:Tl, selenium has a much lower atomic number ($Z = 34$), and the k-absorption edge lies at 13 keV (a very low energy). For the beam energies used in fluoroscopy the x-ray absorption efficiency of a-Se is significantly lower than that of an equivalent thickness of CsI:Tl. In addition, the x-ray absorption efficiency of a-Se falls more rapidly with increasing beam energy than it does with CsI:Tl. Consequently, when used in dynamic detectors the a-Se layer thickness is increased to 1000 μm, from the 500 μm normally used in radiographic versions. Absorption of x-ray photons in the a-Se layer releases electronic charge carriers directly. A bias voltage is applied across the a-Se layer to transfer the charge carriers to the appropriate signal electrode. Due to the high strength of the resulting electric field charge carries rapidly cross the a-Se layer with negligible lateral diffusion. In theory negligible loss of spatial resolution during image capture should benefit image quality; however, in practice fluoroscopic image quality will be degraded due to the effects of noise aliasing.[6] The 2D array of stored charge packets are read out using a mechanism similar to that used in indirect conversion detectors (as described above).

Dynamic, solid-state detectors have a compact, flat-panel construction. A sectional view through a dynamic, solid-state, flat-panel detector (indirect conversion type) is shown in Fig. 1. Components of the detector identified in this figure include the surface light reflector, the CsI:Tl layer, the a-SiH active matrix array, glass substrate plus the refresh light (whose function is explained later). The detector depicted is the Pixium 4800 (Trixell SA, France); this detector was specifically designed for use in cardiac imaging.[16] A working cardiac catheterization laboratory employing this detector is shown in Fig. 2. Recently imaging systems incorporating dynamic, solid-state detectors with larger fields of view (up to 40 cm × 40 cm) have become available. This has broadened the range of clinical applications that can be supported by solid-state detectors to include radiography and fluoroscopy and vascular examinations.[19−25] The vascular imaging system depicted in Fig. 3 incorporates the large-field Trixell Pixium 4700 dynamic detector, (which again exploits indirect conversion). This design of dynamic detectors is incorporated in medical x-ray imaging devices manufactured by Philips Healthcare and Siemens Medical Solutions (in Europe). Other leading manufacturers of dynamic solid-state detector systems include GE Healthcare and Varian Medical Systems (in the USA) and Toshiba Medical Systems and Shimadzu Medical Systems (in Japan). The two former companies utilize indirect-conversion dynamic detectors, whereas the latter two companies use direct-conversion detectors.
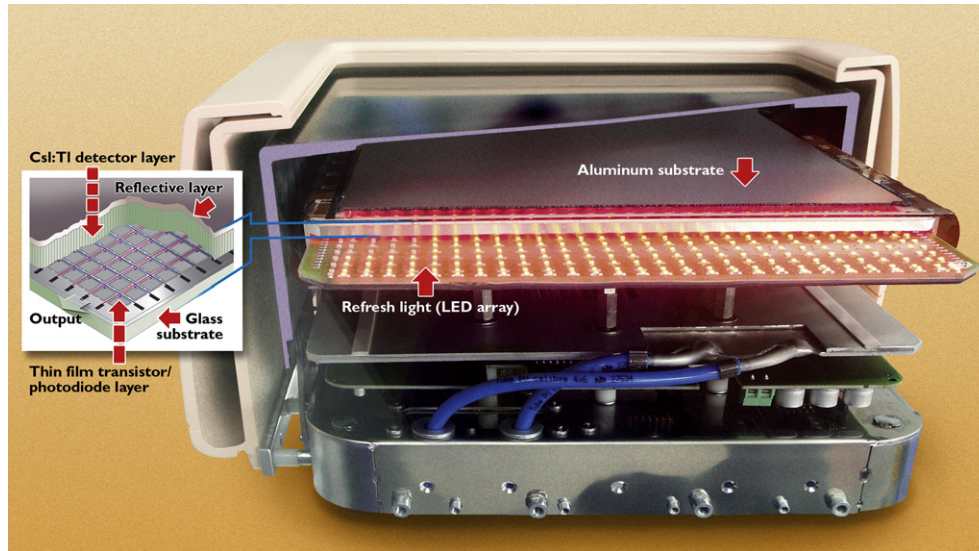
Figure 1 Cross-section through a dynamic, solid-state, flat-panel detector, identifying the surface reflector, CsI:Tl layer, a-SiH active matrix array, and refresh light (Trixell SA Pixium 4800 detector). Reproduced with the permission of Medicamundi.

Physical imaging characteristics

The physical image quality of dynamic digital x-ray image detectors can be evaluated using a toolkit of parameters such as: dynamic range; geometrical distortion, vignetting, and veiling glare; spatial resolution; temporal resolution (lag and memory effect); and detective quantum efficiency (DQE). These parameters are transportable across different designs of x-ray image detector, and can be used to compare imaging system performance on an objective basis.

Dynamic range

The dynamic range of a digital x-ray image detector describes the maximum range of entrance doses over which substantive image information is recorded. In basic terms dynamic range is described by the ratio of the maximum to the minimum detector usable operating dose levels; (specifically the former is defined by the maximum signal capability and the latter by noise). Dynamic x-ray image detectors require a wider dynamic range than DR detectors, as they are multi-

Figure 2 A modern cardiac catheterization laboratory incorporating an Allura Xper FD10 solid-state, cardiac, flat-panel detector in the Yorkshire Heart Centre, Leeds. Reproduced with the permission of Medicamundi.

Figure 3 A modern neurovascular intervention laboratory incorporating a Philips Allura Xper FD20 large-field, dynamic, solid-state detector. Reproduced with the permission of Philips Healthcare.

functional image receptors operating over a wider range of dose levels.[27] For example, modern fluoroscopy demands effective image recording down to dose levels as low as 10 nGy per frame. Where higher quality dynamic images are required exposures are made at between ∼100 nGy and 1 μGy per frame, depending upon the image acquisition mode. The former (lower) value is typical of the dose per frame used in digital cine fluorography, here images are usually acquired at 15 or 30 frames s^{-1}. The latter (higher) dose value is typical of that used in more general applications of digital fluorography. In DSA the dose per frame can approach (or even exceed) radiographic dose levels, *viz.* 10 μGy or greater. In order to accommodate exposure highlights and minimize blooming artefacts, (e.g., over sections of the GI tract containing gas or between the lower limbs during peripheral angiography), detectors must have a maximum dose capability of ∼50–100 μGy. Solid-state detectors have a linear signal response across the dynamic range. The linearity is sufficiently accurate that detectors can support the logarithmic subtraction algorithm used in DSA imaging over a wide dose range.[25] Image signals are normally digitized to 14-bits of grey-scale resolution, (corresponding to 16,384 levels). Solid-state fluoroscopy detectors reportedly offer a dynamic range some 10 times greater than x-ray IITV fluoroscopy systems.[28] The wide dynamic range and excellent contrast rendition of indirect conversion dynamic solid-state detectors can be gauged from the double-contrast barium enema study shown in Fig. 4.

Geometry, vignetting, and veiling glare

X-ray IITV channels are susceptible to a number of field-dependent defects that can degrade the cosmetic quality of fluoroscopic and fluorographic images. Geometrical distortion arises from the electron-optical design of the x-ray image-intensifier tube. The mapping of electrons from a concave photocathode onto a planar output screen results in a form of geometrical distortion known as pincushion distortion. The degree of pincushion distortion exhibited by a large-field x-ray image intensifier is illustrated in Fig. 5a. Pincushion distortion reflects a progressive increase in geometrical magnification towards the periphery of the image field. At the same time the luminance of the image field falls, producing a non-uniform distribution in brightness (or vignetting). Image intensifiers are also subject to a second form of geometrical distortion, due to extraneous magnetic fields, known as S-distortion. The impact of S-distortion on image quality is

Figure 4 A double-contrast barium enema image acquired with a large-field dynamic solid-state flat-panel detector. Figure courtesy of Sue Rimes.

compounded by the fact that it varies with changing angulation of the C-arm; this is felt most strongly in rotational angiography and related reconstructive imaging applications. Solid-state detectors are subject to none of these forms of geometrical distortion, and therefore, consistently record images with excellent field homogeneity as shown in Fig. 5b. As solid-state detectors are insensitive to magnetic fields they can be successfully implemented in hybrid x-ray/magnetic resonance (MR) imaging laboratories[29] or in conjunction with magnetic catheter navigation equipment.[27]

Images produced by x-ray IITV systems are subject to a loss of contrast due to the large-area scatter of x-rays, electrons, and light, which occurs at the various stages of image conversion. The overall effect of such scatter mechanisms on the recorded image contrast is known as veiling glare. Veiling glare is often quantified in terms of the low frequency drop (LFD), which is derived from the modulation transfer function (MTF). MTF is the concept often used to describe the spatial resolution properties of x-ray imaging systems.[6] LFD measures the deterioration in MTF directly attributable to large-area scatter mechanisms. The greater the value of LFD the poorer the reproduction of large-area contrast will be, and vice-versa. Solid-state detectors exhibit a much smaller LFD than x-ray IITV systems, typically by a factor of
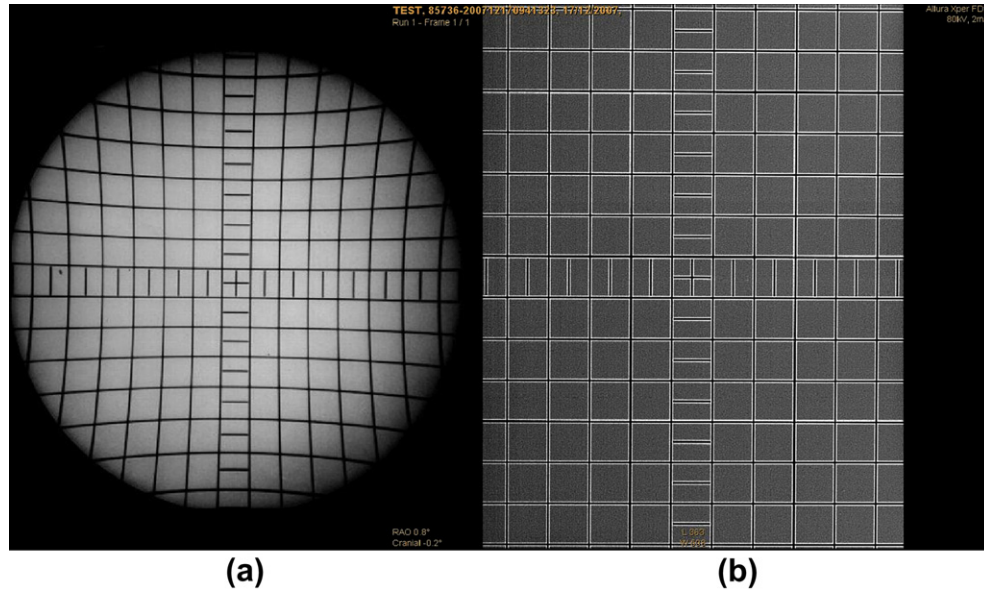
Figure 5   Comparison of the geometrical distortion exhibited by a large-field x-ray image intensifier (a), compared with the distortion-free image of a large-field, dynamic, solid-state detector (b). Figure courtesy of Pat Turner.

between five and 10.[21] Consequently, dynamic, solid-state detectors produce images with superior contrast and wider dynamic range than x-ray IITV systems; this is reflected in the excellent reproduction of the high-contrast structures depicted in Fig. 4.

Spatial resolution

The spatial resolution of a solid-state detector is affected by a number of physical and technical factors. These include light scatter in the x-ray absorption layer (in the case of indirect-conversion devices), the detector pixel sampling interval and aperture size, and the bandwidth of the readout electronics. Dynamic, solid-state, flat-panel detectors come in a variety of sizes, form factors and pixel resolutions, matched to their target clinical application(s). Typical values of spatial imaging characteristics for indirect-conversion dynamic detectors designed for cardiac, vascular, and radiography and fluoroscopy applications are listed

in Table 1 (Readers should note that relevant characteristics, including pixel sampling interval and Nyquist frequency, were defined in a previous review.[6]). Equivalent values for a large-field digital x-ray IITV system are included for reference. The maximum spatial resolution of a large-field, dynamic, solid-state detector exceeds that of the digital x-ray IITV system by a factor of over two. It should be noted that the spatial resolution of digital x-ray IITV systems deteriorates toward the periphery of the image field. The spatial resolution of solid-state detectors is maintained throughout the whole field of view. Dynamic, solid-state detectors offer multiple (sometimes up to five) ancillary zoom-field selections. These zoom-fields are used to magnify the presented image and, therefore, improve the resolution of fine-detail structures (albeit for a reduced field of view). The spatial resolution of solid-state detectors remains essentially constant, independent of the field size selected. The frame rate of a dynamic solid-state detector can be increased, say from 15 to

Table 1   Typical spatial imaging characteristics of dynamic, solid-state detectors designed for three clinical application areas, compared with a digital IITV system (results are quoted for the largest field selection in each case)

	Cardiac detector	Vascular detector	Radiography and fluoroscopy detector	Digital IITV
Maximum field of view (cm)	Square field 24.8 × 24.8	Rectangular field 38.2 × 29.4	Square field 42.6 × 42.6	Circular field 35 cm diameter
Pixel sampling interval (μm)	184	154	148	341
Maximum pixel array	956 × 954	2480 × 1910	2880 × 2881	1024 × 1024
Nyquist frequency (lp/mm)	2.72	3.25	3.38	1.46

30 or from 30 to 60 frames s^{-1} by sacrificing spatial resolution and/or field coverage. In a detector's largest field mode this is usually achieved by binning (averaging) data over blocks of [2 × 2] or [4 × 4] pixels. For a digital x-ray IITV system the spatial resolution falls markedly as the field of view is increased. The spatial resolution of a large-field, solid-state detector can be gauged from the abdominal DSA image of the superior mesenteric artery presented in Fig. 6. The vascular bed is depicted with excellent detail resolution across the whole image field.

Lag and ghosting

In a fluoroscopy examination of the GI tract structures can move with a velocity of between 10 and 30 mm s^{-1} due to peristalsis.[30] In cardiac angiography the mean velocity of a coronary vessel[31] is typically ~50 mm s^{-1}, while the peak velocity can exceed 100 mm s^{-1}. Fluoroscopy detectors, therefore, must be able to record images with sufficient temporal resolution to meet the needs of their target examination(s). The temporal resolution of a dynamic solid-state image detector is defined by two physical mechanisms[32]: memory effect (or ghosting) and lag. These effects occur concurrently; under a given set of circumstances a detailed experimental analysis is required to distinguish and quantify their individual contributions.

Memory effect refers to the production of a spurious frozen pattern (a so-called ghost image), which mirrors the image content produced by the preceding x-ray exposure. This phenomenon can persist for some time (even several minutes) particularly after an intense x-ray exposure of a high-contrast structure is made.[33] Both indirect and direct-conversion detectors are susceptible to memory effect, but they occur due to differing physical mechanisms. In general, the latter design of detector is more susceptible to ghosting
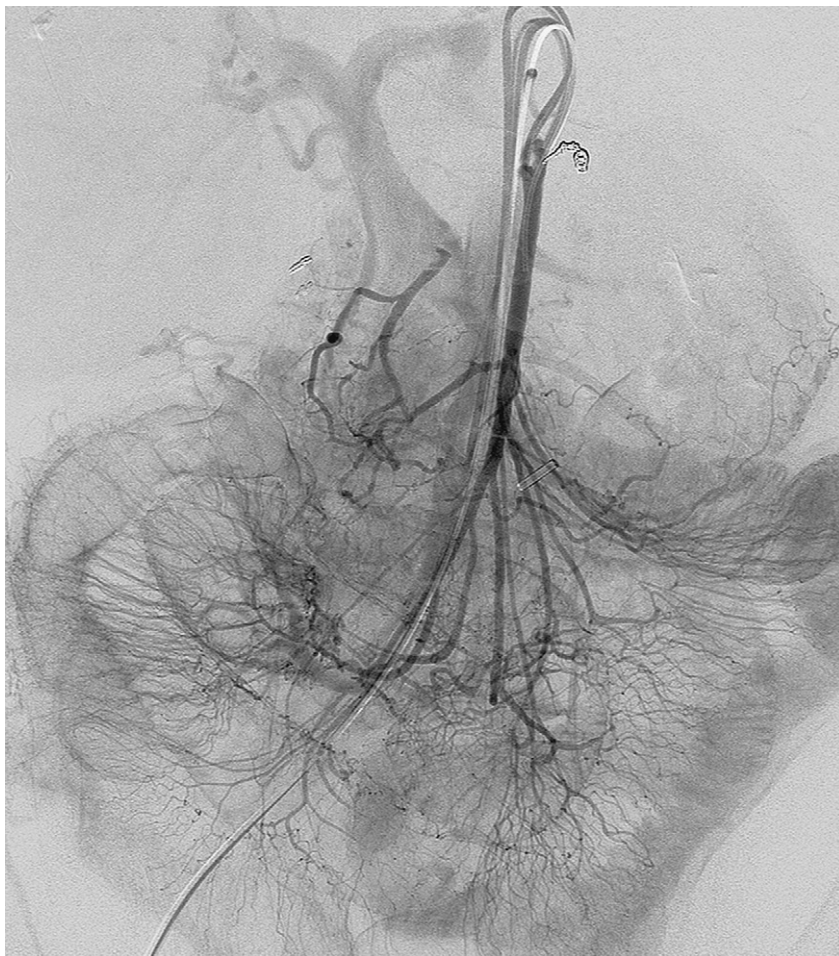

Figure 6 Abdominal DSA image of superior mesenteric artery acquired with a large-field, dynamic, solid-state detector. Figure courtesy of Anne Allington, and Drs Raman Uberoi and Phil Boardman.

artefacts.[32] Memory effect reflects a non-uniform variation in detector response depending upon the exposure history. With regard to indirect-conversion detectors, memory effect represents an increase in CsI:Tl light emission and a-Si:H photodiode gain, following the x-ray exposure. These effects manifest themselves as a spurious increase in detector conversion efficiency, producing a so-called bright-burn artefact in images acquired subsequently. Conversely, in direct-conversion detectors memory effect reflects a reduction (fatigue) in photoconductor response. Memory effect can be a particular problem in mixed-mode imaging applications, specifically where low-dose fluoroscopy might follow immediately after an image is acquired at a high fluorographic dose level, e.g., as occurs in DSA.[27] The x-ray dose per frame during fluoroscopy can be as low as one thousandth of that used during serial image acquisition; therefore, even a modest degree of memory effect may intrude upon the fluoroscopic images that follow.

Lag is the property that quantifies the ability of an image detector to accurately record time-varying changes in image content; the larger the lag, the poorer the temporal response and vice versa. Lag results from the carry-over of a proportion of recorded signal content into succeeding frames in the sequence. In the case of indirect-conversion detectors a small contribution of lag arises from afterglow in the CsI:Tl layer, (but this is rarely significant in routine fluoroscopy). In practice, lag largely results from the relatively slow temporal response of a-Si:H. More specifically lag arises from the trapping and subsequent slow release (de-trapping) of charge carriers in the photodiode array.[34] In direct-conversion detectors lag is compounded by charge trapping/de-trapping mechanisms in the a-Se photoconductor.[32] Without correction lag causes unacceptable unsharpness (smearing) of rapidly moving and time-varying image structures.

Dynamic solid-state detectors incorporate measures to minimize lag and memory effect. Many modern dynamic detectors achieve this using a so-called refresh (or reset) light, which reconditions the detector prior to each new image acquisition cycle.[9,20,28,34] The refresh light usually takes the form of an array of light-emitting diodes (see Fig. 1), which floods the detector with light photons, saturating charge-trapping sites in the a-Si:H prior to each x-ray exposure. As a result, lag (and memory effect) is reduced to an acceptably low level ensuring a suitably fast detector response. Signal retention due to lag in a modern indirect conversion detector is reportedly as low

as 0.3% at a time 1 s after termination of the x-ray exposure; after 10 s the lag reduces by a further order of magnitude.[27] This ensures that the temporal resolution is adequate for high-speed imaging applications, such as paediatric cardiac fluoroscopy. Equivalent lag figures for direct conversion detectors are reportedly higher.[27] In some clinical applications a moderate degree of lag can be tolerated, and is used to improve fluoroscopic image quality by time-averaging (smoothing) noise fluctuations. Depending upon the type of clinical application, a suitable degree of lag is normally synthesized using digital recursive filtering.

DQE

DQE is the most effectual physical parameter used to quantify and compare the performance of different x-ray image detectors objectively.[35] To simplify the discussion, here it is assumed that the fluoroscopic image detector exhibits zero lag, (or any lag that does exist is fully corrected). The DQE of the detector can then be defined by the ratio,[6,35]

$$DQE_{detector} = SNR^2_{recorder}/SNR^2_{input}$$

Where SNR^2_{input} is the square of the signal-to-noise ratio at the input of the image detector. This is defined by the fluence of x-ray photons (number per unit area) contributing to an individual frame in the fluoroscopic image sequence. $SNR^2_{recorded}$ is the square of the signal-to-noise ratio recorded by the image detector. The value of $SNR^2_{recorded}$ can be computed from the output data. In terms of counting statistics $SNR^2_{recorded}$ is an estimate of the fluence of information carriers that the recorded image frame is actually worth.

The information content of a recorded image frame can never exceed that delivered to the detector in the incident x-ray beam, therefore,

$$0 \leq DQE_{detector} \leq 1$$

A DQE of unity implies that the recording of x-ray image information by the detector is perfect. At the other extreme a DQE of zero implies that no information at all is recorded. Real-world x-ray image detectors obviously offer a DQE value falling somewhere between these two extremes. The deterioration in recorded information is for two principal reasons. First, no detector can absorb all the incident x-ray photons with 100% efficiency. Inevitably some x-ray photons pass straight through the x-ray absorber, while others that are absorbed may then be re-emitted and escape the detector. This loss in primary information is compounded by any noise sources arising in the detector itself (e.g.,
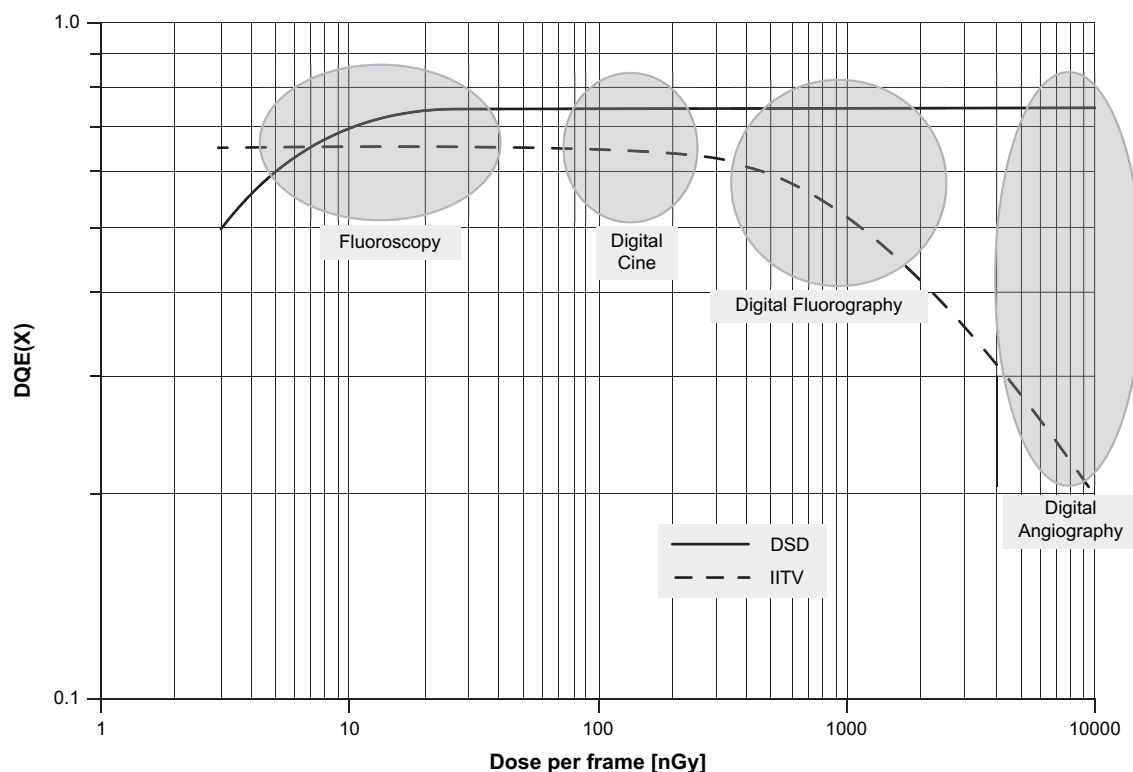
Figure 7 Variation of DQE as a function of the detector entrance dose-per-frame, comparing the performance of a (indirect conversion) dynamic, solid-state detector with a digital IITV system.

electronic noise arising in the a-Si:H matrix array and the readout circuitry). The DQE of a modern, indirect-conversion, dynamic, solid-state detector falls in the range 0.7—0.75.[16,19,36] In the case of direct-conversion detectors noise-aliasing plays a significant part in degrading DQE.[6,37] The DQE of a direct conversion dynamic solid-state detector typically lies in the range 0.5—0.6.[38]

The influence of electronic noise on detector DQE performance is strongly dependent on signal level (and, therefore, detector entrance dose per frame); and this is an important characteristic of dynamic detector performance. This can be analysed by measuring how DQE varies as a function of detector entrance dose per frame. In early designs of dynamic solid-state fluoroscopy detectors the image quality fell below that of digital x-ray IITV systems; this was due to the comparatively large contribution of electronic noise at that time.[7,10,11,39] Typical DQE performance for a modern indirect-conversion, solid-state, dynamic detector is shown in Fig. 7. Equivalent results for a modern digital x-ray IITV system have been included for reference. The dose ranges used in standard fluoroscopy, digital cine acquisition (as commonly used in cardiac angiography), digital fluorography (serial imaging) and (non-subtractive)

vascular imaging (where the dose-per-frame may reach those used in radiography) are delineated for reader orientation. The high DQE of the indirect conversion detector is maintained across the majority of the dynamic range. The DQE performance is 10—15% greater than that of an IITV-based digital fluoroscopy system.[40,41] This suggests that an improvement in image quality, and/or saving in patient/staff dose, should be feasible if this design of solid-state detector is used. This proposition has been verified in cardio-angiography[42] and cardiac electrophysiology imaging, respectively.[43] In modern indirect-conversion detectors good DQE performance can be maintained during fluoroscopy down to dose levels of less than 10 nGy per frame.[16,19,36] At exceptionally low dose levels (say well below 5 nGy per frame) digital x-ray IITV systems still offer better imaging performance; however, such dose levels would rarely be used in clinical routine. At higher dose levels, say 1 μGy per frame and above, a marked deterioration in x-ray IITV system DQE occurs, and the superiority of the dynamic, solid-state detectors is apparent. This fall in DQE results from the growing influence of the (noisy) granular structure of the II input and output phosphor screens. This acts as a residual fixed-pattern noise source, which

becomes more pronounced as the x-ray quantum noise diminishes with increasing dose. In solid-state detectors fixed-pattern noise is eliminated during system calibration, and this holds across the dynamic range. Overall the graphs presented in Fig. 7 confirm that modern, indirect-conversion, dynamic, solid-state detectors are dose-efficient imaging devices, which can support the full spectrum of clinical applications previously underwritten by digital x-ray IITV systems.

New directions in digital fluoroscopy

3D-enhanced fluoroscopy

The 1990s saw a growth in the use of digital x-ray IITV systems in 3D reconstruction imaging, based upon a rotating C-arm imaging geometry.[44] Before clinically acceptable reconstructions can be computed, extensive data processing is required to correct for defects such as the changing geometrical distortion (which occurs as the image intensifier rotates around the patient).[45] For reasons explained above dynamic, solid-state detectors essentially produce distortion-free image data. Consequently, these new detectors yield 3D image reconstructions with greater detail resolution[46,47] and fewer artefacts.[48,49] 3D reconstruction imaging is typically used to improve the visualization of complex bone structures during orthopaedic surgery[50] or a tortuous network of blood vessels in endovascular procedures.[47] Reportedly the latter can aid the clinician in navigating and deploying interventional devices, thereby reducing procedure times and patient/staff radiation dose.[47,51] The availability of dynamic solid-state detectors now makes it possible to reconstruct 3D (and 2D sectional) images of not only high contrast details, but also soft-tissue structures of comparatively low subject contrast[52]; (digital x-ray IITV systems lack the contrast resolution and dynamic range required to reliably achieve the latter). To illustrate the quality of 3D reconstructive imaging achievable with a solid-state detector let us focus on the technique known as "dynamic 3D road-mapping".[53,54] This visualization tool makes it possible to project (and automatically register) the live 2D fluoroscopy image upon a 3D reconstruction of relevant vasculature, (and when useful, a CT-like sectional slice through the surrounding soft-tissue). A 3D roadmap composition of the iliac arteries (with a catheter *in situ*) acquired using a dynamic solid-state detector is presented in Fig. 8. 3D-enhanced digital fluoroscopy is set to proliferate and increase in clinical utility, for example, incorporating real-time interventional procedure evaluation and device tracking.[55] Such advances will facilitate the increasingly sophisticated and precise interventions that will be realized in the future.
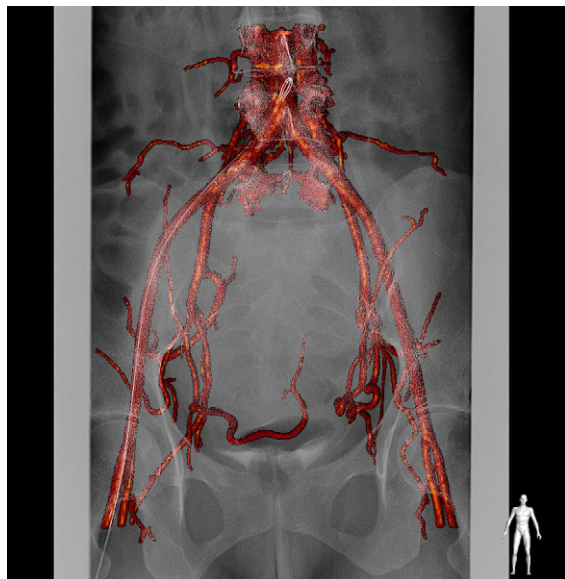

Figure 8 3D roadmap image of the iliac arteries with the catheter *in situ* acquired using a dynamic, solid-state detector. Reproduced with the permission of Philips Healthcare.

Increasing detector sensitivity

Further innovations in basic dynamic solid-state detector design are anticipated. These possibly include increases in detector sensitivity, by boosting signal gain and/or reducing electronic noise. Solutions considered include modifying the architecture of the readout array to maximize the pixel fill-factor[56] and implementing signal amplification at a pixel-level.[57] In the future signal digitization is likely to be increased to 16 bit grey-scale resolution (and in time possibly higher) to improve detector performance in 3D reconstructive imaging applications. Automatic switching of the amplifier gain setting can also be used to extend detector dynamic range in these applications.[58] It is conceivable that direct-conversion dynamic detectors might mature to the point where they can challenge, or even out-perform indirect-conversion detectors. This could follow the adoption of more efficient x-ray photoconductive converter materials than a-Se, such as poly-crystalline HgI_2, PbI_2 or PbO.[59,60] Reportedly, however, significant

refinement of the physical properties of these materials would be required before this is likely to happen.[61]

Alternative readout arrays

Despite the success of a-Si:H-based dynamic detector arrays, alternative forms of electronic readout have been mooted. For example, several authors have speculated that readout electronics might be better fabricated from crystalline silicon wafers, typically in the form of C-MOS (complementary metal oxide semi-conductor) technology.[27,61–63] Such readout arrays could be fabricated in semiconductor plants set up to manufacture C-MOS wafers for commodity products, possibly leading to reductions in detector manufacturing costs. In addition, such dynamic detectors might afford performance enhancements, including improved spatial and temporal resolution plus higher image acquisition rates.[62] C-MOS is also well-suited to the implementation of complex component structures in the detector array itself rather than as external circuitry. Resulting pixel-level processing functions might include automatic gain control, array timing, adaptive digital image enhancement, or more exotic concepts, such as x-ray photon counting (to maximize DQE) or energy-selective (viz, colour) x-ray imaging.[27,61] Consequently, adoption of C-MOS might conceivably lead to more economic detector designs, potentially combined with enhanced dynamic, functional, and 3D imaging capabilities.

Conclusions

Dynamic, solid-state image detectors have reached full technological maturity; early deficiencies, such as moderate image quality at low dose rates, excessive dark current and artefacts due to lag and memory effect having been resolved. An x-ray IITV system comprises a complex chain of electron-optical components, which are subject to drifts and variations in adjustment over time, which can degrade clinical performance. Solid-state digital detectors are inherently more stable image acquisition platforms, which (in principle) require minimal quality assurance monitoring. The cosmetic quality of dynamic solid-state detectors is excellent with zero geometrical distortion and vignetting, immunity from blooming (at exposure highlights) and negligible contrast loss due to internal scatter mechanisms. These detectors exhibit a wider dynamic range and retain high spatial

resolution when imaging over larger fields of view. They are also insensitive to magnetic fields and can, therefore, be successfully implemented in mixed x-ray/MR imaging laboratories or where magnetic catheter-navigation equipment is used. The image quality of an x-ray IITV system can vary markedly across the field of view. Indeed optimum imaging performance only really occurs within a quality area of limited extent. For solid-state detectors the quality area encompasses the whole field of view. Solid-state, flat-panel detectors are lighter and less bulky than x-ray image intensifier TV systems, affording better accessibility to the patient and greater anatomical coverage. The DQE of modern indirect-conversion detectors is greater than that of both x-ray IITV systems and direct-conversion detectors, and offers high-quality fluoroscopic imaging down to commendably low dose rates. Dynamic, solid-state detectors can support the full range of fluoroscopy-guided procedures, including cardiac and vascular (DSA) imaging, radiography and fluoroscopy procedures and mobile surgical imaging. The transition from IITV to solid-state detector-based digital fluoroscopy now looks irrevocable. Dynamic solid-state detectors are extremely versatile x-ray image acquisition devices supporting fluoroscopy, serial image acquisition, and 3D reconstructive imaging; the latter benefiting from the greater geometrical integrity of the acquired data. Combining 3D visualization with fluoroscopy will prove increasingly influential in interventional radiology. Investigations into ways of improving the technical performance of solid-state detectors are still on-going. The longer term might conceivably see the migration from a-Si:H to C-MOS based readout electronics. Such a re-alignment in dynamic, solid-state detector design might ease manufacturing costs, while encouraging further innovations in dynamic x-ray imaging.

Acknowledgements

Radiographer), and Drs Raman Uberoi and Phil Boardman (Consultant Radiologists) of the Vascular Angiography Department at the John Radcliffe Hospital, Oxford, who kindly provided Fig. 6. Dr Drazenko Babic, Clinical Scientist at Philips Healthcare (in the Netherlands), who kindly provided Fig. 8.

References

1. Krohmer JS. Radiography and fluoroscopy, 1920 to the present. *RadioGraphics* 1989;**9**:1129–53.
2. Schueler BA. General overview of fluoroscopic imaging. *RadioGraphics* 2000;**20**:1115–26.
3. Van Lysel MS. Fluoroscopy: optical coupling and the video system. *RadioGraphics* 2000;**20**:1769–86.
4. Mistretta CA, Crummy AB. Diagnosis of cardiovascular disease by digital subtraction angiography. *Science* 1981;**214**:761–5.
5. Pooley RA, McKinney JM, Miller DA. Digital fluoroscopy. *RadioGraphics* 2001;**21**:521–34.
6. Cowen AR, Kengyelics SM, Davies AG. Solid-state flat-panel digital radiography detectors and their physical imaging characteristics. *Clin Radiol* 2008;**63**:487–98.
7. Schiebel U, Conrads N, Jung N, et al. Fluoroscopic x-ray imaging with amorphous silicon thin-film arrays. *SPIE Proc Phys Med Imaging* 1994;**2162**:129–40.
8. Antonuk LE, Yorkston J, Huang W, et al. A real-time, flat-panel amorphous silicon digital x-ray imager. *RadioGraphics* 1995;**15**:993–1000.
9. Chabbal J, Chaussat T, Ducourant T, et al. Amorphous silicon x-ray image sensor. *SPIE Proc Phys Med Imaging* 1996;**2708**:499–510.
10. Colbeth RE, Allen MJ, Day DJ, et al. Characterisation of an amorphous silicon fluoroscopic imager. *SPIE Proc Phys Med Imaging* 1997;**3032**:42–51.
11. Colbeth RE, Allen MJ, Day DJ, et al. Flat panel imaging system for fluoroscopy applications. *SPIE Proc Phys Med Imaging* 1998;**3338**:376–87.
12. Bruijns TJ, Alving PL, Baker EL, et al. Technical and clinical results of an experimental flat dynamic (digital) x-ray image detector (FDXD) systems with real-time correction. *SPIE Proc Phys Med Imaging* 1998;**3336**:33–44.
13. Bury RF, Cowen AR, Davies AG, et al. Initial experiences with an experimental solid-state universal digital x-ray detector. *Clin Radiol* 1998;**53**:923–8.
14. Bruijns AJC, Bury R, Busse F, et al. Technical and clinical assessments of an experimental flat dynamic x-ray image detector system. *SPIE Proc Phys Med Imaging* 1999;**3659**:324–35.
15. Jung N, Alving PL, Busse F, et al. Dynamic x-ray imaging based on an amorphous silicon thin-film array. *SPIE Proc Phys Med Imaging* 1998;**3336**:974–85.
16. Busse F, Rutten W, Sandkamp B, et al. Design and performance of a high quality cardiac flat panel detector. *SPIE Proc Phys Med Imaging* 2002;**4682**:819–27.
17. Granfors PR, Albagli D, Tkaczyk JE, et al. Performance of a flat cardiac detector. *SPIE Proc Phys Med Imaging* 2001;**4320**:77–86.
18. Sivananthan UM, Moore J, Cowan JC, et al. A flat-detector cardiac cath lab system in clinical practice. *Medicamundi* 2004;**48**:4–12.
19. Granfors PR, Aufrichtig R, Possin GE, et al. Performance of a 41 × 41 cm² amorphous silicon flat panel x-ray detector designed for angiographic and R&F imaging applications. *Med Phys* 2003;**30**:2715–26.
20. Ducourant T, Michel M, Vieux G, et al. Optimization of key building blocks for a large area radiographic and fluoroscopic dynamic x-ray detector based on a-Si:H/CsI:Tl flat panel technology. *SPIE Proc Phys Med Imaging* 2000;**3977**:14–25.
21. Bruijns AJC, Bastiaens R, Hoornaert B, et al. Image quality of a large-area dynamic flat detector: comparison with a state-of-the-art IITV system. *SPIE Proc Phys Med Imaging* 2002;**4682**:332–43.
22. Colbeth RE, Boyce S, Fong R, et al. 40 × 30 cm² flat imager for angiography, R&FG and cone-beam CT applications. *SPIE Proc Phys Med Imaging* 2001;**4320**:94–102.
23. Choquette M, Demers Y, Shukri Z, et al. Real time performance of a selenium based detector for fluoroscopy. *SPIE Proc Phys Med Imaging* 2001;**4320**:501–8.
24. Tousignant O, Demers Y, Laperriere L, et al. Clinical performances of a 14''×14'' real time amorphous selenium flat panel detector. *SPIE Proc Phys Med Imaging* 2003;**5030**:71–6.
25. Ducourant T, Couder D, Wirth T, et al. Image quality of digital subtraction angiography using flat detector technology. *SPIE Proc Phys Med Imaging* 2003;**5030**:203–14.
26. Neitzel U. Recent technological developments and their influence. *Radiat Prot Dosimetry* 2000;**90**:15–20.
27. Spahn M. Flat detectors and their clinical applications. *Eur Radiol* 2005;**15**:1934–47.
28. Seibert JA. Flat-panel detectors: how much better are they? *Pediatr Radiol* 2006;**36**:173–81.
29. Fahrig R, Wen Z, Ganguly A, et al. Performance of a static-anode/flat-panel x-ray fluoroscopy system in a diagnostic strength magnetic field: truly hybrid x-ray/MR imaging system. *Med Phys* 2005;**32**:1775–84.
30. Nguyen TC, Rowlands JA. A study of motion in gastro-intestinal x-ray fluoroscopy. *Med Phys* 1989;**16**:569–76.
31. Achenbach S, Ropers D, Holle J, et al. In-plane coronary arterial motion velocity: measurement with electron-beam CT. *Radiology* 2000;**216**:457–63.
32. Zhao W, DeCresenzo G, Rowlands JA. Investigation of lag and ghosting in amorphous selenium flat-panel x-ray detectors. *SPIE Proc Phys Med Imaging* 2003;**4682**:9–20.
33. Siewerdsen JH. Jaffray. DA A ghost story: spatio-temporal response characteristics of an indirect-detection flat-panel imager. *Med Phys* 1999;**26**:1624–41.
34. Overdick M, Solf T, Wischmann H-A. Temporal artefacts in flat dynamic x-ray detectors. *SPIE Proc Phys Med Imaging* 2001;**4320**:47–58.
35. Dainty JC, Shaw R. *Image science*. London: Academic Press; 1975.
36. Tognina CA, Mollov I, Yu JM, et al. Design and performance of a new a-Si flat panel imager for use in cardiovascular and mobile C-arm imaging systems. *SPIE Proc Phys Med Imaging* 2004;**5368**:648–56.
37. Moy JP. Signal-to-noise ratio and spatial resolution in x-ray electronic imagers: is the MTF a relevant parameter? *Med Phys* 2000;**27**:86–93.
38. Tousignant O, Demers Y, Laperriere L, et al. Spatial and temporal image characteristics of a real-time large area a-Se x-ray detector. *SPIE Proc Phys Med Imaging* 2005;**5745**:207–15.
39. Davies AG, Cowen AR, Kengyelics SM, et al. Threshold contrast detail detectability measurement of the fluoroscopic image quality of a dynamic solid-state digital x-ray image detector. *Med Phys* 2001;**28**:11–5.

40. Spekowius G, Boerner H, Eckenbach W, et al. Simulation of the imaging performance of x-ray image intensifier YV camera chains. *SPIE Proc Phys Med Imaging* 1995;**2432**:12–23.

41. Baker EL, Cowen AR, Kemner R, et al. A physical evaluation of a CCD-based x-ray image intensifier fluorography system for cardiac applications. *SPIE Proc Phys Med Imaging* 1998;**3336**:430–41.

42. Vano E, Geiger B, Schreiner A, et al. Dynamic flat panel detector versus image intensifier in cardiac: dose and image quality. *Phys Med Biol* 2005;**50**:5731–42.

43. Davies AG, Cowen AR, Kengyelics SM, et al. X-ray dose reduction in fluoroscopically guided electrophysiology procedures. *Pacing Clin Electrophysiol* 2006;**29**:262–71.

44. Fahrig R, Fox AJ, Lownie S, et al. Use of a C-arm system to generate true three-dimensional computed rotational angiograms: preliminary *in vitro* and *in vivo* results. *AJNR Am J Neuroradiol* 1997;**18**:1507–14.

45. Fahrig R, Moreau M. Holdsworth. Three dimensional computed tomographic reconstruction using a C-arm mounted XRII: correction of image intensifier distortion. *Med Phys* 1997;**24**:1097–106.

46. Baba R, Konno Y, Ueda K, et al. Comparison of flat-panel detector and image-intensifier detector for cone-beam CT. *Comput Med Imaging Graph* 2002;**26**:153–8.

47. Hirota S, Nakao N, Yamamoto S, et al. Cone-beam CT with flat-panel detector digital angiography system: early experiences in abdominal interventional procedures. *Cardiovasc Intervent Radiol* 2006;**29**:1034–8.

48. Hirai T, Korogi Y, Ono K, et al. Pseudostenosis phenomenon at volume-rendered three-dimensional digital angiography of intracranial arteries: frequency, location and effect on image evaluation. *Radiology* 2004;**232**:882–7.

49. Kakeda S, Korogi Y, Ohnari N, et al. 3D digital subtraction angiography of intracranial aneurysms: comparison of flat panel detector with conventional image intensifier TV system using a vascular phantom. *AJNR Am J Neuroradiol* 2007;**28**:839–43.

50. Akpek S, Brunner T, Benndorf G, et al. Three-dimensional imaging and cone beam volume CT in C-arm angiography with flat panel detector. *Diagn Interv Radiol* 2005;**11**:10–3.

51. Hatakeyama Y, Kakeda S, Korogi Y, et al. Intracranial 2D and 3D DSA with flat panel detector of the direct conversion type: initial experience. *Eur Radiol* 2006;**16**:2594–602.

52. Heran NS, Song JK, Mamba K, et al. The utility of DynaCT in neurovascular procedures. *AJNR Am J Neuroradiol* 2006;**27**:330–2.

53. Soderman M, Babic D, Homan R, et al. 3D roadmap in neuro-angiography: technique and clinical interest. *Neuroradiology* 2005;**47**:735–40.

54. Wilhelm K, Babic D. 3D angiography in the interventional clinical routine. *Medicamundi* 2006;**50**:24–31.

55. Racadio JM, Babic D, Homan R, et al. Live 3D guidance in the interventional radiology suite. *AJR Am J Roentgenol* 2007;**189**:357–64.

56. Weisfield RL, Yao W, Speaker T, et al. Performance analysis of a 127 micron pixel large-area TFT photo-diode array with boosted fill factor. *SPIE Proc Phys Med Imaging* 2004;**5368**:338–48.

57. Matsura N, Zhao W, Huang Z, et al. Digital radiology using active matrix readout: amplified pixel detector array for fluoroscopy. *Med Phys* 1999;**26**:672–81.

58. Roos PG, Colbeth RE, Mollov I, et al. Multiple-gain-ranging readout method to extend the dynamic range of amorphous silicon flat-panel imagers. *SPIE Proc Phys Med Imaging* 2004;**5368**:139–49.

59. Street RA, Ready SE, van Schuylenbergh K, et al. Comparison of PbI$_2$ and HgI$_2$ for direct detection active matrix x-ray image sensors. *J Appl Phys* 2002;**91**:3345–55.

60. Kasap SO, Rowlands JA. Direct-conversion flat-panel x-ray image sensors for digital radiography. *Proc IEEE* 2002;**90**:591–604.

61. Neitzel U. Status and prospects of digital detector technology for CR and DR. *Radiat Prot Dosimetry* 2005;**114**:32–8.

62. Nakagawa K, Mizuno S, Aoki Y, et al. C-MOS flat-panel sensor for real-time x-ray imaging. *Radiat Med* 2000;**18**:349–53.

63. Graeve T, Weckler GP. High-resolution C-MOS imaging detector. *SPIE Proc Phys Med Imaging* 2001;**4320**:68–76.